

A real-time performance improvement method for composite time scale

Fangmin Wang(王芳敏), Wenlin Li(李汶林), Hongfei Dai(戴鸿飞), Chunyi Li(李春怡), Jianhua Zhou(周建华), Shenhui Xue(薛申辉), and Bo Wang(王波)

Citation: Chin. Phys. B, 2024, 33 (**9**): 090601. DOI: 10.1088/1674-1056/ad6131
Journal homepage: http://cpb.iphy.ac.cn; http://iopscience.iop.org/cpb

What follows is a list of articles you may be interested in

Physics package based on intracavity laser cooling ^{87}Rb atoms for space cold atom microwave clock

Siminda Deng(邓思敏达), Wei Ren(任伟), Jingfeng Xiang(项静峰), Jianbo Zhao(赵剑波), Lin Li(李琳), Di Zhang(张迪), Jinyin Wan(万金银), Yanling Meng(孟艳玲), Xiaojun Jiang(蒋小军), Tang Li(李唐), Liang Liu(刘亮), and Desheng Lü(吕德胜)
Chin. Phys. B, 2024, 33 (**7**): 070602. DOI: 10.1088/1674-1056/ad4bc1

Proposal for a realtime Einstein-synchronization-defined satellite virtual clock

Chenhao Yan(严晨皓), Xueyi Tang(汤雪逸), Shiguang Wang(王时光), Lijiaoyue Meng(孟李皎悦), Haiyuan Sun(孙海媛), Yibin He(何奕彬), and Lijun Wang(王力军)
Chin. Phys. B, 2024, 33 (**7**): 070601. DOI: 10.1088/1674-1056/ad3dc9

A redundant subspace weighting procedure for clock ensemble

Hai Xu(徐海), Yu Chen(陈煜), Mo-Chi Liu(刘默驰), and Yu-Zhuo Wang(王玉琢)
Chin. Phys. B, 2024, 33 (**4**): 040601. DOI: 10.1088/1674-1056/ad1b43

Coherent optical frequency transfer via 972-km fiber link

Xue Deng(邓雪), Xiang Zhang(张翔), Qi Zang(臧琦), Dong-Dong Jiao(焦东东), Dan Wang(王丹), Jie Liu(刘杰), Jing Gao(高静), Guan-Jun Xu (许冠军), Rui-Fang Dong(董瑞芳), Tao Liu(刘涛), and Shou-Gang Zhang(张首刚)
Chin. Phys. B, 2024, 33 (**2**): 020602. DOI: 10.1088/1674-1056/ad0629

Robust free-space optical frequency transfer in time-varying link distances conditions

Zhou Tong(童周), Lei Liu(刘雷), Jia-Liang Wang(王家亮), Qian Cao(操前), Zhi-Cheng Jin(金志成), Kang Ying(应康), Shen-Sheng Han(韩申生), Zheng-Fu Han(韩正甫), and You-Zhen Gui(桂有珍)
Chin. Phys. B, 2024, 33 (**2**): 020601. DOI: 10.1088/1674-1056/ad0718

A real-time performance improvement method for composite time scale

Fangmin Wang(王芳敏)[1,2], Wenlin Li(李汶林)[1,2], Hongfei Dai(戴鸿飞)[1,2], Chunyi Li(李春怡)[1,2], Jianhua Zhou(周建华)[3], Shenhui Xue(薛申辉)[3], and Bo Wang(王波)[1,2,†]

[1] *State Key Laboratory of Precision Space–time Information Sensing Technology, Department of Precision Instrument, Tsinghua University, Beijing* 100084, *China*

[2] *Key Laboratory of Photonic Control Technology (Tsinghua University), Ministry of Education, Beijing* 100084, *China*

[3] *Beijing Satellite Navigation Center, Beijing* 100094, *China*

(Received 12 February 2024; revised manuscript received 25 June 2024; accepted manuscript online 10 July 2024)

The composite time scale (CTS) provides a stable, accurate, and reliable time scale for modern society. The improvement of CTS's real-time performance will improve its stability, which strengths related applications' performance. Aiming at this goal, a method achieved by determining the optimal calculation interval and accelerating adjustment stage is proposed in this paper. The determinants of the CTS's calculation interval (characteristics of the clock ensemble, the measurement noise, the time and frequency synchronization system's noise and the auxiliary output generator noise floor) are studied and the optimal calculation interval is obtained. We also investigate the effect of ensemble algorithm's initial parameters on the CTS's adjustment stage. A strategy to get the reasonable initial parameters of ensemble algorithm is designed. The results show that the adjustment stage can be finished rapidly or even can be shorten to zero with reasonable initial parameters. On this basis, we experimentally generate a distributed CTS with a calculation interval of 500 s and its stability outperforms those of the member clocks when the averaging time is longer than $\sim$ 1700 s. The experimental result proves that the CTS's real-time performance is significantly improved.

Keywords: composite time scale, real-time performance, calculation interval, adjustment stage

PACS: 06.30.Ft, 06.20.–f **DOI:** 10.1088/1674-1056/ad6131

1. Introduction

Precise time have extensive applications in diverse fields, such as satellite navigation,[1,2] geodesy,[3,4] power grid management,[5,6] telecommunication,[7] gravitational wave detection,[8] and tests of fundamental physics.[9–11] To generate and maintain a stable and reliable time scale, the composite time scale (CTS) is widely adopted by worldwide timekeeping institutions due to its obvious advantages in stability and reliability.[12,13]

The CTS has two realizations, paper CTS, and physical CTS. The paper CTS, also named as paper clock, is calculated with a clock ensemble using an ensemble algorithm. It can be employed to steer an auxiliary output generator (AOG) whose input signal is from the master clock to generate the physical CTS. Meanwhile, in terms of real-time performance, the CTSs can be classified into real-time ones and deferred ones. The distinction between them mainly lies in whether their paper realizations can be calculated based on the measured comparison data of clock ensemble in real-time. In order to further introduce the state of the art in CTS and describe the concern in this paper, we would like to clarify some key concepts of CTS. The calculation interval refers to the generation interval of the paper CTS. The adjustment interval refers to the frequency steering period to realize the physical CTS, which is generally equal to the calculation interval. The effective time, an evaluation index of the physical CTS, refers to the averaging time when the CTS's stability outperforms those of member clocks. Since the physical CTS is always realized by deferred frequency adjustment, the effective time is definitely longer than the calculation interval.[14]

The CTS uses weights to adjust the relationship between member clocks, i.e., the relationship of noise within the clock ensemble and reduces the noise by reasonably weighting on them.[15] When the averaging time is longer than the calculation interval, CTS's stability is improved and outperforms those of member clocks.[12,13] Different calculation intervals represent noise at different scales being averaged within the clock ensemble, determining when the stability bonus for the weighted average of the clock ensemble works. Meanwhile, the calculation interval is a direct indicator of CTS's real-time performance. It can be seen that CTS's stability and real-time performance are closely linked through the calculation interval. Hence, choosing the optimal calculation interval to improve the CTS's real-time performance will also make the stability bonus for the weighted average of the clock ensemble work at a shorter averaging time, which means that CTS's stability is improved at a shorter averaging time. This will further enhance the performance of related applications.

[†]Corresponding author. E-mail: bo.wang@tsinghua.edu.cn

© 2024 Chinese Physical Society and IOP Publishing Ltd

However, owing to the link noise introduced in time and frequency transfer process, the distributed CTSs based on widely employed satellite synchronization links usually require a calculation interval of more than one day.[16–19] Thanks to the high-precision fiber based time and frequency synchronization technique, a distributed real-time CTS with a calculation interval of 1200 s has been demonstrated in 2019. Its stability outperforms those of member clocks when the averaging time is longer than $\sim$ 5000 s.[17] Even based on a co-located clock ensemble, that means no link noise, to our knowledge, the CTS with shortest calculation interval is achieved by NIST's AT1 and UTC(NIST), whose calculation intervals are 720 s. The calculation interval here is chosen mostly for computational convenience, since it is an exact decimal fraction of an hour.[20,21] So the question arises, is it possible to further improve the real-time performance of the CTS? What is the boundary for the choice of the calculation interval?

On the other hand, the ensemble algorithm often requires an adjustment stage at startup, which generally takes several days. During the period, parameters of the ensemble algorithm needs to be iterated to reasonable levels. The generated CTS in this stage does not enter the steady state. This will lead to a great waste of experimental time, as the data during this stage would not be usable for evaluating the CTS's performance. Likewise, the ensemble algorithm goes through a similar adjustment stage again when new member clocks are introduced to the clock ensemble. In fact, the adjustment stage can be considered as another indicator of the CTS's real-time performance. Further accelerating the adjustment stage so that the CTS can be stabilized as rapidly as possible is important for the improvement of the real-time performance. Actually, the real-time performance of the CTS is also related to the stability of the master clock, which has been proved in our previous work.[14] We mainly focus on effects of the calculation interval and the adjustment stage on the real-time performance of CTS.

In this paper, we propose a real-time performance improvement method for the CTS. It is achieved by determining the optimal calculation interval and accelerating CTS's adjustment stage. First, we analyze the determinants of paper CTS's calculation interval, which mainly include the characteristics of the clock ensemble, the measurement noise and the time and frequency synchronization system's noise. On the basis, the restrictions of the AOG noise floor on CTS's effective time is clarified. This restriction in turn gives an optimal calculation interval. Then, a strategy to accelerate the adjustment stage by reasonably configuring the initial parameters of the ensemble algorithm is developed. The CTS's adjustment stages are compared when the strategy is used and not used. The results show that the adjustment stage can be finished rapidly or even can be shorten to zero with reasonable initial parameters. Finally, a distributed CTS with a calculation interval of 500 s (the optimal calculation interval identified by the analysis) is built to experimentally demonstrate the method. It has been running continuously over 7 days. The CTS's effective time is obtained as $\sim$ 1700 s, which indicates a significant improvement in real-time performance compared to the existing CTS and validates the effectiveness of the proposed method.

The rest of this paper is organized as follows. Section 2 analyzes the determinants of CTS's calculation interval and gives a way to determine an optimal calculation interval. In Section 3, we develop a strategy to get the reasonable initial parameters of the ensemble algorithm and carry out a simulation demonstration. Section 4 summaries the implementation procedure of the proposed method and takes an experiment to verify the method. Finally, Section 5 concludes this paper.

2. Improve CTS's real-time performance by determining the optimal calculation interval

In this section, we will clarify the principle of deriving an optimal calculation interval and demonstrate it through a simulation. Since the physical CTS is realized through frequency steering according to the paper CTS, the analysis will focus on the generation progress of both paper CTS and physical realization.

2.1. Determinants of paper CTS's calculation interval

The property of the paper CTS is mainly determined by both the clock ensemble and ensemble algorithm. Among the ensemble algorithms, the weighted average ensemble algorithm is the most common method.[22,23] Here, we take AT1, a widely used real-time weighted average ensemble algorithm, to analyze the determinants of paper CTS's calculation interval.[24,25]

Generally, the phase time difference of atomic clock is modeled as a quadratic polynomial combined with stochastic noise, which can be defined as[26]

$$x(t+T) = x(t) + y(t)\,T + \frac{1}{2}dT^2 + \xi, \tag{1}$$

where $x(t)$ and $y(t)$ represent the phase time difference and fractional frequency difference of atomic clock at time epoch t, respectively; d is the frequency drift of the clock; T represents the time interval of the measured phase time difference used to calculate the paper CTS, which is also the calculation interval of the paper CTS; ξ is the stochastic noise in the phase time difference originated from the measurement noise of the phase comparator (PCO), H-maser's noises, as well as the time and frequency synchronization system. In the AT1 algorithm, the average fractional frequency difference of the clock over

the interval, $y(t+T)$, would be estimated by[26]

$$y(t+T)=\frac{x(t+T)-x(t)}{T}. \tag{2}$$

To correctly estimate the frequency difference of the clock, a proper calculation interval needs to be chosen. There are two criteria to be fulfilled in determining the calculation interval. The first criterion requires that the calculation interval is long enough so that the contribution of the clock's fractional frequency difference to the measured phase time difference is larger than ξ. It can be expressed as

$$y\cdot T\gg\xi. \tag{3}$$

In our system, the measurement noise of the PCO is smaller than 1×10^{-13} s. The phase fluctuation originated from H-maser is also smaller than 1×10^{-13} s at the averaging time of the calculation interval smaller than 1 d. The phase fluctuation originated from time and frequency synchronization system is smaller than 1×10^{-14} s. Hence, it is obtained as $\xi\leq10^{-13}$ s. y is 1×10^{-13} (typical fractional frequency difference of an H-maser is generally on the order of 10^{-13}). On this basis, the minimum calculation interval is given by $T\gg1$ s. Meanwhile, the other criterion requires that the calculation interval should be short enough so that the contribution of the frequency drift to the measured phase time differences is smaller than ξ, and smaller than the contribution of the clock's fractional frequency difference. It can be expressed as

$$\frac{1}{2}d\cdot T^2\ll\xi. \tag{4}$$

Here, d is 1×10^{-21} s^{-1} in our system, which is also the typical frequency drift for an H-maser. The criterion gives a range of calculation interval as $T\ll10^4$ s. Therefore, after considering the measurement noise, the time and frequency synchronization system's noise and the characteristics of the clock ensemble, a loose range of the calculation interval is derived, which is $1\text{ s}\ll T\ll10^4$ s.

2.2. Influence of the calculation interval on paper CTS's stability

The stability and real-time performance of the CTS are closely linked through calculation interval. Inherently, the weighted average ensemble algorithm reduces the noise of the CTS by reasonably weighting on noises of the member clocks. The average level of clock noises, which directly affects the paper CTS's stability, is related with the calculation intervals. Hence, we carry out simulations to explore the influence of the calculation interval on the paper CTS's stability after obtaining the range of the calculation interval. In the simulation, a 40-day phase time data of 4 simulated H-masers and AOG noise floor with a time interval of 1 s are used. The dominant noise of the data is white frequency modulation (WFM), white phase modulation (WPM), and flicker frequency modulation (FFM). Their simulative parameters are obtained by piecewise fitting the individual stability curves of the H-masers and AOG noise floor in our CTS system and given in our previous work.[14] The stabilities of simulated clock ensemble and the AOG noise floor are shown in Fig. 1(a), where clock C is the most stable clock.

Using the AT1 algorithm, the paper CTSs with different calculation intervals are calculated and their stabilities are presented in Fig. 1(b). The results are individual stabilities of CTSs respect to an ideal clock, which is calculated based on the phase time sequence of the CTS with respect to an ideal clock, marked as $x_{\rm c}$. At time epoch t, $x_{\rm c}(t)$ can be obtained by directly adding the CTS, $x_{\rm cr}(t)$, to the master clock, $x_{\rm r}(t)$, which can be expressed as

$$x_{\rm c}(t)=x_{\rm cr}(t)+x_{\rm r}(t). \tag{5}$$

Here, $x_{\rm cr}(t)$ is the phase time differences between the CTS and the master clock; $x_{\rm r}(t)$ is the simulated phase time difference of the master clock with respect to an ideal clock. Besides, the stability results of paper CTSs and physical CTSs obtained in simulations of Sections 2 and 3 are all individual stabilities calculated in a similar way. Meanwhile, we also estimate approximately the CTS's stability limit (also shown in Fig. 1(b)) by directly weighted averaging the individual stabilities of the member clocks at different averaging time. It can be expressed as[27]

$$\sigma^2_{\rm CTS}(\tau)=\sum_{i=1}^{4}\omega_i^2(\tau)\,\sigma_i^2(\tau), \tag{6}$$

where $\sigma_{\rm CTS}(\tau)$ and $\sigma_i(\tau)$ represent the Allan deviation of the CTS and clock i at the averaging time of τ, respectively; $\omega_i(\tau)$ is the weight of the clock i at the averaging time of τ, which is calculated based on the inverse of the Allan variance $\sigma_i^2(\tau)$ of each member clock and can be formulated as

$$\omega_i(\tau)=\frac{1/\sigma_i^2(\tau)}{\sum\limits_{i=1}^{4}1/\sigma_i^2(\tau)}. \tag{7}$$

The weight has been proved to be the optimal weight of the member clock for the CTS.[28]

By comparing the stabilities of the member clocks in Fig. 1(a) and those of the paper CTSs with different calculation intervals in Fig. 1(b), we can see that when the averaging time is longer than paper CTS's respective calculation interval, all paper CTSs outperform the member clocks. Furthermore, it can be seen from Fig. 1(b) that the paper CTSs' stabilities with different calculation intervals are almost identical when the averaging time is longer than corresponding calculation interval. This proves the feasibility to improve the CTS's real-time performance with a short calculation interval. Compared

with the CTS's stability limit, the paper CTSs' stabilities with different calculation intervals remain similar to it, also qualifying the correctness of the paper CTS calculation. Based on the results, in subsequent sections, we will use the stability of the paper CTS with a 10-s calculation interval to represent the stability level of the paper CTS under the clock ensemble configuration.

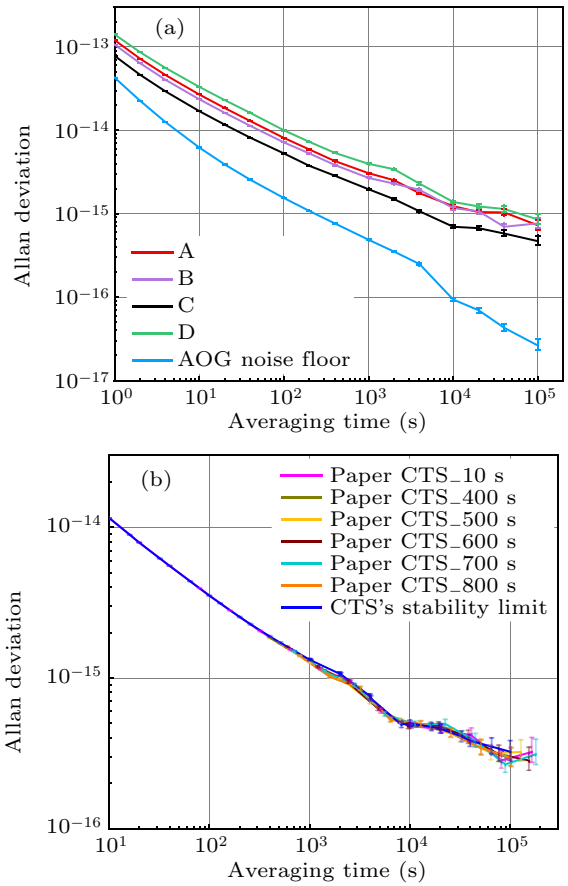


Fig. 1. Individual stabilities of the simulated clocks, the CTS's stability limit and paper CTSs with different calculation intervals. (a) Stability curves of simulated H-maser ensemble and AOG noise floor, where clock C is the most stable; A, B, C, and D: simulated H-masers. (b) Stability curves of paper CTSs with different calculation intervals and the CTS's stability limit; Paper CTS_10 s represents paper CTS with a calculation interval of 10 s, other legends have similar meanings.

2.3. Limitations of AOG noise floor on CTS's calculation interval

In the physical realization process of the CTS, the AOG is a key instrument, whose output is the physical CTS. The input frequency of the AOG is from the master clock, and the output frequency of AOG is steered by the paper CTS. However, the noise floor of AOG will affect the accuracy of the frequency adjustment and deteriorate the stability of physical CTS. Therefore, an adequate adjustment interval is needed to smooth the AOG noise to ensure that the frequency fluctuation arising from the noise is small enough to be ignored. We analyze the limitations of AOG noise floor on CTS's calculation interval (equal to the adjustment interval) based on the simulated data in Subsection 2.2.

It can be seen in Fig. 1(a) that AOG noise floor is more stable than the H-masers in the clock ensemble at all averaging times, which is the case where the AOG is placed in an ideal environment. In Fig. 2, by subtracting the stability of paper CTS (the pink line) from that of the most stable clock-C (the black line), the stability improvement expectation is obtained (the brown line). Actually, it is more reasonable to obtain the stability improvement expectation by calculating the square root of difference between paper CTS stability square and clock-C stability square. The stability improvement expectation here represents the stability bonus for the weighted average of the clock ensemble. It refers to the stability improvement level of the paper CTS, as well as the desired level of the physical CTS's stability improvement. Subsequently, comparing the stability improvement expectation and the stability of the AOG noise floor (the blue line), we can obtain the lower boundary of physical CTS's effective time as ~ 50 s (exactly the intersection of the two curves). When the averaging time is longer than 50 s, the effect of the weighted average of the clock ensemble appears, otherwise the stability bonus for the weighted average of the clock ensemble is obscured by the AOG noise floor. It means that for the CTS system configuration, no matter how short the calculation interval is chosen, the stability of the physical CTS can only outperform those of member clocks when the averaging time is longer than ~ 50 s.

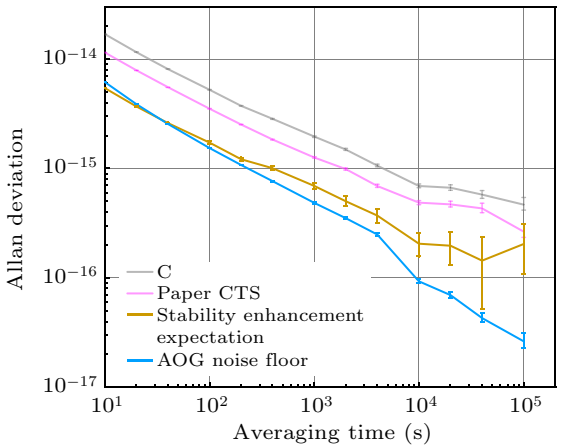


Fig. 2. Simulation results of the limitation of the AOG noise floor on the CTS's effective time. The paper CTS represents the stability of paper CTS with a calculation interval of 10 s in Fig. 1(b). The stability improvement expectation is obtained by subtracting the individual stability of paper CTS's stability and that of the most stable clock within the clock ensemble-clock C.

In the actual experimental situation, the noise floor of AOG will be affected by temperature fluctuation of the environment. Especially, the periodic temperature fluctuation (exactly the situation where our CTS is generated) will seriously deteriorate the stability of the AOG noise floor. This will in turn affect the lower boundary of the physical CTS's effective time. We will simulate this effect according to following parameters.

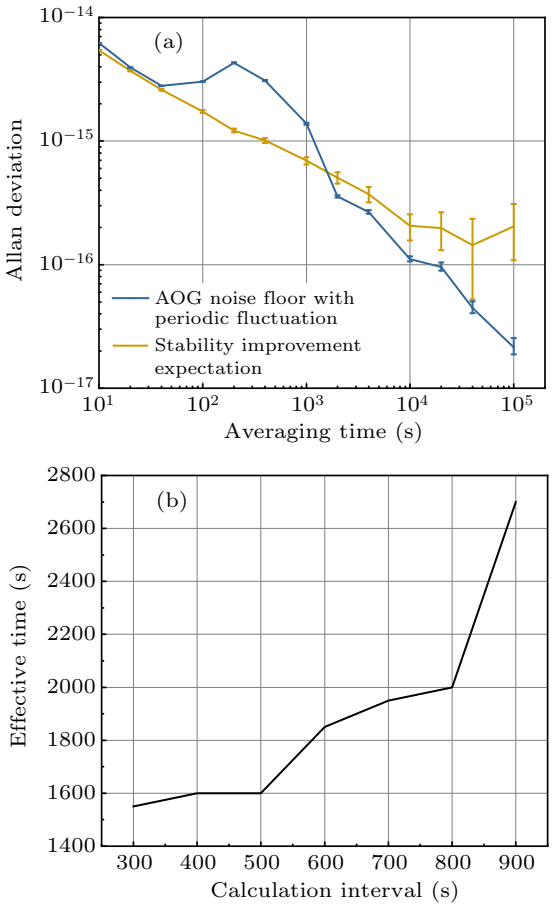


Fig. 3. Simulation results of the limitation of the AOG noise floor with periodic fluctuation on the CTS's effective time. (a) Stability curves of the AOG noise floor with periodic fluctuation and that of stability improvement expectation. (b) The effective time of the CTSs with different calculation intervals.

The AOG noise floor with periodic fluctuation is simulated with a magnitude of 6×10^{-15} and period of 678 s. These parameters are derived from the real-measured AOG noise floor of our CTS system with the method in Ref. [29]. The other parameters of stochastic noise in the AOG noise floor are the same as in Ref. [14]. Its stability curve is shown in Fig. 3(a).

It can be seen from Fig. 3(a) that the AOG noise floor's stability here is larger than the stability improvement expectation until the averaging time of $\sim$ 1600 s. Consequently, the lower boundary of the effective time significantly increases to $\sim$ 1600 s. To derive the optimal calculation interval for the effective time of 1600 s, we need to first estimate the possible values of the calculation interval. As a result of the deferred frequency steering in the CTS's physical realization, the calculation interval must be shorter than the effective time. Hence, the corresponding calculation interval should be on the order of hundreds of seconds. Base on the analysis, the physical CTSs with a calculation interval of 300 s, 400 s, 500 s, 600 s, 700 s, 800 s, 900 s are simulated respectively. Their corresponding effective time are shown in Fig. 3(b). The results show that the CTS with a calculation interval of 500 s corresponds to an effective time of 1600 s. When the calculation intervals are shorter than 500 s, their effective time remains identical, which is close to 1600 s. When the calculation interval is longer than 500 s, the corresponding effective time increases with the calculation interval. The optimal calculation interval is finally chosen as $\sim$ 500 s.

3. Improve CTS's real-time performance by accelerating adjustment stage

Normally, the initial parameters of the ensemble algorithm are arbitrarily set to the empirical values. This will result in a long adjustment stage before CTS entering the steady state. To accelerate the adjustment stage, it is necessary to reasonably configure the initial parameters of the ensemble algorithm. As the reasonable parameters need to be obtained by calculating the paper CTS, a piece of clock ensemble historical comparison data is required. Here, we still use the simulated data in Subsection 2.2 for analysis and demonstration. First, through setting the empirical values as the initial parameters, we calculate a paper CTS and record the iterative values of the corresponding parameters. The paper CTS data is then truncated into successive segments and their individual stabilities are calculated separately to identify when the adjustment stage ends. So far, when the CTS entering the steady state, any set of iterative values of the parameters can be used as the reasonable initial parameters. The parameters whose initial values need to be reasonably configured in AT1 algorithm include the weight of the member i clock—ω_i, the predicted phase time difference between the CTS and the i clock—$\hat{x}_{i-a}$, and the fractional frequency difference between the CTS and the i clock—y_{i-a}. Table 1 gives a specific example of applying the proposed strategy to obtain reasonable initial parameters based on empirical initial parameters. The simulative results of CTSs using two sets of initial parameters are compared in Fig. 4.

It can be seen from Fig. 4(a) that it takes $\sim$ 5 d for the parameter ω_i with the empirical initial value to be iterated to a reasonable level. For the parameter with the reasonable initial value in Fig. 4(b), the iterative adjustment stage is accelerated to $\sim$ 1 d. Figures 4(c) and 4(d) show that for the parameter y_{i-a}, the iterative adjustment stage is $\sim$ 4 d with the empirical initial value, while iterative adjustment stage's duration can be reduced to zero with the reasonable initial value. The stability results in Fig. 4(e) reveal that with the empirical initial parameters, the CTS undergoes an adjustment stage of $\sim$ 5 d at the startup of the ensemble algorithm. However, with reasonable initial parameters, the adjustment stage almost disappears. This means that the CTS would skip the adjustment stage and be stabilized from the beginning. In this way, CTS's adjustment stage can be greatly accelerated.

Table 1. Initial parameters of the AT1 ensemble algorithm used in the simulation.

Parameters	ω_i	$\hat{x}_{i-a}$	y_{i-a}
Empirical initial parameters	[0.25, 0.25, 0.25, 0.25]	[0, 0, 0, 0]	[0, 0, 0, 0]
Reasonable initial parameters	[0.19, 0.20, 0.22, 0.39]	$[1.22\times10^{-7}, -1.25\times10^{-7}, -1.25\times10^{-7}, 4.03\times10^{-8}]$	$[4.43\times10^{-13}, -4.54\times10^{-13}, -4.53\times10^{-13}, 1.46\times10^{-13}]$

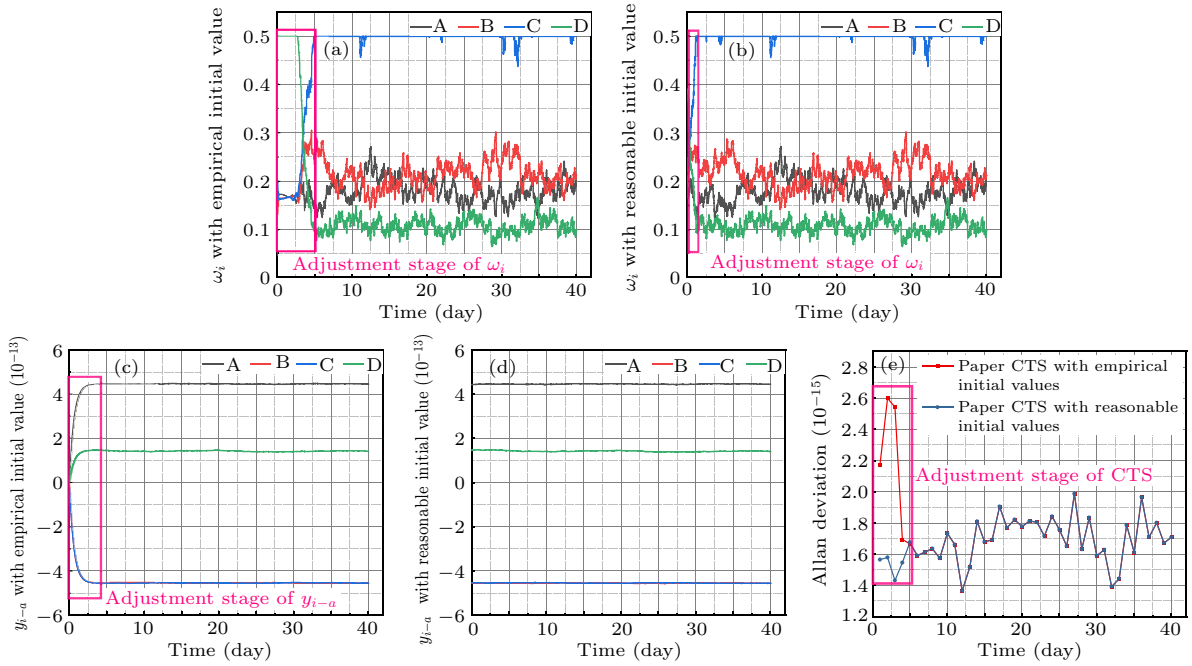


Fig. 4. Simulative results of CTSs with the empirical and reasonable initial parameters. Panels (a) and (b) are the iterative values of the ω_i with the empirical initial value and the reasonable initial value, respectively; panels (c) and (d) are the iterative values of the y_{i-a} with the empirical initial value and the reasonable initial value, respectively; panel (e) is the stability results of paper CTSs with the empirical and reasonable initial parameters.

4. Method and experimental demonstration

Based on the analyses in Sections 2 and 3, we summarize the implementation procedures of the method to improve the CTS's real-time performance in this section. It consists of three parts and its flow diagram is shown in Fig. 5.

In the first part, a piece of clock ensemble comparison data is needed as an important prior basis. In addition, the PCO's measurement noise, the time and frequency synchronization system's noise and AOG noise floor also need to be obtained in advance. The second part aims at optimizing the calculation interval based on the data gained in the first part. It has four steps: (i) determine the fractional frequency difference and the frequency drift of the clock ensemble; (ii) obtain a loose range of the calculation interval using the two criteria from the ensemble algorithm; (iii) calculate the individual stability of the paper CTS, and derive the CTS's stability improvement expectation by subtracting the individual stability of paper CTS from that of the best member clock; Then, evaluate the lower boundary of the physical CTS's effective time by comparing the stability improvement expectation with the AOG noise floor. (iv) Estimate the optimal calculate interval for the lower boundary of the effective time and test them with physical realization. On this basis, the optimal calculation interval (500 s in our simulation and experimental demonstration) is got for the CTS system configuration. It is necessary to noticed that in the simulations of Section 2, the individual stabilities of CTS and member clocks can be calculated directly based on the phase difference of the simulated clock ensemble data respected to an ideal clock. Nevertheless, with the real-measured comparison data of atomic clocks, individual stability estimation methods, such as the three-cornered-hat and N-cornered-hat methods described in Refs. [30,31] are required to calculate the individual stabilities of the paper CTS and physical CTS as well as those of member clocks in steps (iii) and (iv). After that, the obtained optimal calculation interval will be transferred to the third part as a parameter to accelerate the adjustment stage. There are three steps in this part: (i) calculate the paper CTS with the optimal calculation interval and empirical initial parameters based on the clock ensemble comparison data; (ii) find a set of iterative values of the parameters when the paper CTS entering the steady state; (iii) choose the obtained values as the reasonable initial parameters of ensemble algorithm and use the optimal calculation interval to generate a physical CTS. In this way, a CTS with improved real-time performance can be achieved.

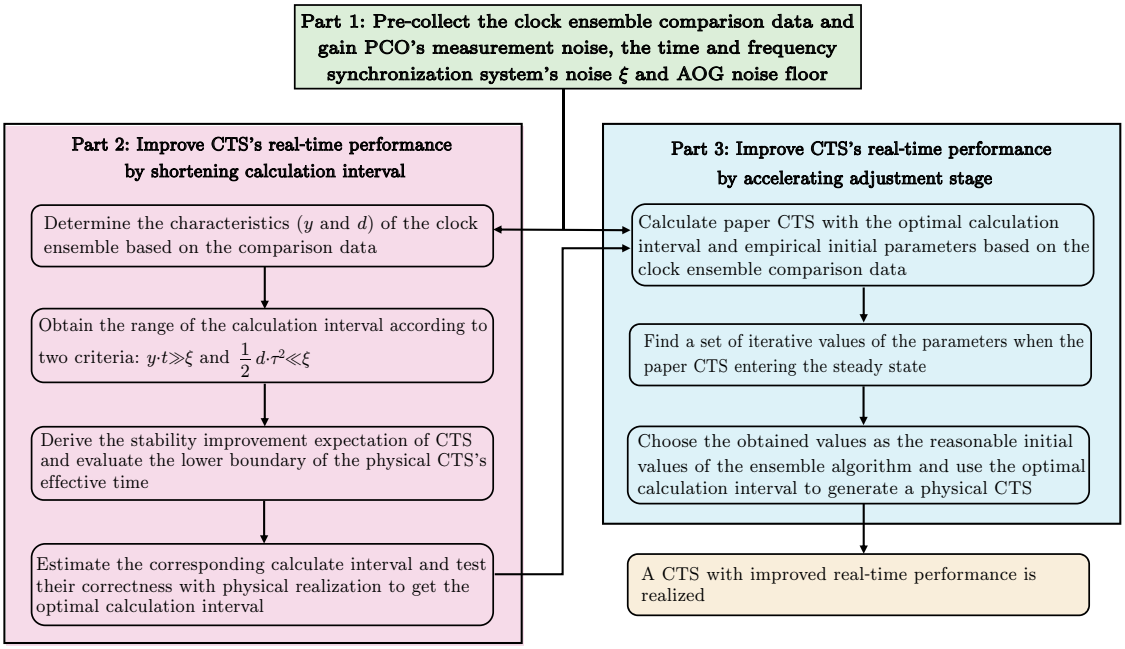


Fig. 5. Flow diagram of the method to improve the CTS's real-time performance.

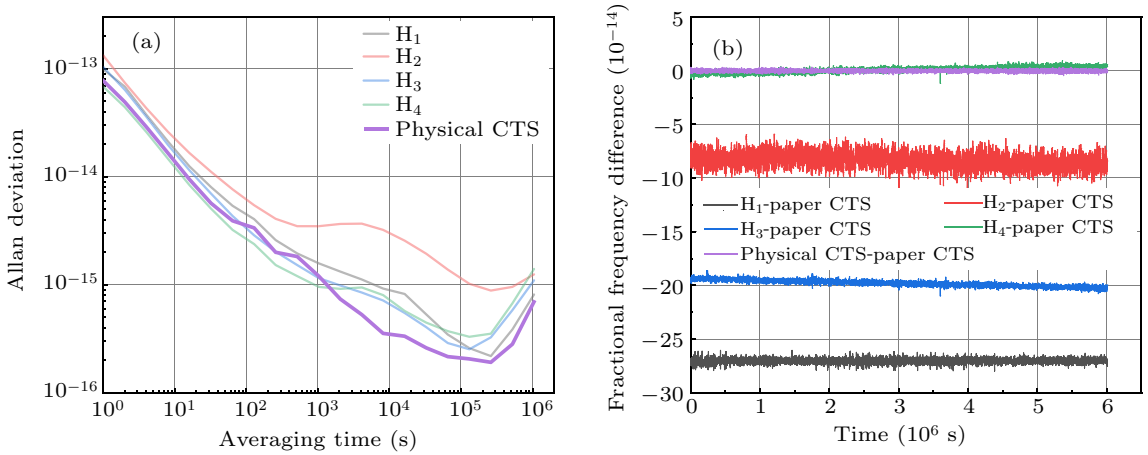


Fig. 6. Experimental results of the experimental physical CTS with 500-s calculation interval. (a) Individual stability of the experimental physical CTS measured by the N-Cornered-Hat method. H_1, H_2, H_3, and H_4: H-masers from different institutions. (b) The relative fractional frequency difference of member clocks and physical CTS with respect to the paper CTS; H_1-Paper CTS represents the fractional frequency difference of clock H_1 with respect to the paper CTS, other legends have similar meanings.

Based on the Beijing regional time and frequency synchronization network, a 70 days continuous test is carried out.[14,17,32] Four H-masers (denoted as H_1, H_2, H_3, and H_4) from four different institutions in the network are incorporated to generate the CTS. Among them, H_1, H_3, and H_4 are the remote H-masers from Beijing Satellite Navigation Center, Beijing Institute of Radio Metrology and Measurement, National Institute of Metrology, China, respectively, while H_2 is the local H-maser from Tsinghua University. They are connected through the commercial fiber links with the fiber-based frequency synchronization technique introduced in Ref. [33]. The length of fiber links is 26 km between H_1 and H_2, 21 km between H_3 and H_2, and 39 km between H_4 and H_2, respectively. Thanks to the high frequency transmission stability of the technique, three remote H-maser signals are recovered at Tsinghua University stably and in real time. The recovered remote signals are then compared with the local H-maser with a PCO. The phase time difference data derived from PCO are used for the paper CTS calculation in a computer. An AOG referenced by a remote master clock (H_4) which is the most stable clock in the ensemble is finally controlled by the computer to generate the physical CTS. The calculation interval of the CTS is 500 s. The results are shown in Fig. 6.

Figure 6(a) gives the individual stability of the experimental physical CTS measured by the N-Cornered-Hat method. It can be seen that the stability of the physical CTS outperforms those of the member clocks when the averaging time is longer than $\sim$ 1700 s. It conforms to the simulative results in Fig. 3(b). In the meanwhile, figure 6(b) shows the relative fractional frequency difference of member clocks and

physical CTS with respect to the paper CTS. We can see that the frequency noise and frequency drift of the physical CTS are decreased compared with those of the member clocks. The real-time performance of the CTS is obviously improved compared with that of distributed CTS reported in Refs. [14,17].

5. Conclusion

In this paper, we propose a method to improve CTS's real-time performance through determining the optimal calculation interval and accelerating CTS's adjustment stage. We give the determinants of the CTS's calculation interval, including the characteristics of the clock ensemble, the measurement noise, the time and frequency synchronization system's noise, and the AOG noise floor. We further provide a way to determine an optimal calculation interval. Based on this, the effect of the ensemble algorithm's initial parameters is studied. It shows that with reasonable initial parameters, the CTS's adjustment stage can be finished rapidly or even can be reduced to zero. To get the reasonable initial parameters, we develop a strategy and demonstrate it with a simulation. Finally, a distributed CTS with a calculation interval of 500 s is generated. The results reveal that the stability of the CTS outperforms those of the member clocks when the averaging time is longer than $\sim$ 1700 s and the real-time performance of the CTS is significantly improved.

Acknowledgements

Project supported in part by the National Key Research and Development Program of China (Grant No. 2021YFA1402102), the National Natural Science Foundation of China (Grant No. 62171249), and the Fund by Tsinghua University Initiative Scientific Research Program.

References

[1] Han C H, Yang Y X and Cai Z W 2011 *Metrologia* **48** S213
[2] Tavella P and Petit G 2020 *Satell. Navig.* **1** 10
[3] Lisdat C, *et al.* 2016 *Nat. Commun.* **7** 12443
[4] McGrew W F, Zhang X, Fasano R J, Schaffer S A, Beloy K, Nicolodi D, Brown R C, Hinkley N, Milani G, Schioppo M, Yoon T H and Ludlow A D 2018 *Nature* **564** 87
[5] Zhang Z H, Gong S P, Dimitrovski A D and Li H S 2013 *IEEE Trans. Smart Grid* **4** 87
[6] Moussa B, Debbabi M and Assi C 2016 *IEEE Commun. Surv. Tutor.* **18** 1952
[7] Levine J 2011 *Metrologia* **48** S203
[8] Kolkowitz S, Pikovski I, Langellier N, Lukin M D, Walsworth, R L and Ye J 2016 *Phys. Rev. D* **94** 124043
[9] Takamoto M, Ushijima I, Ohmae N, Yahagi T, Kokado K, Shinkai H and Katori H 2020 *Nat. Photon.* **14** 411
[10] Matsakis D 2016 *IEEE International Frequency Control Symposium*, May 9–12, New Orleans, LA, USA, p. 6
[11] Peil S, Crane S, Hanssen J L, Swanson T B and Ekstrom C R 2013 *Phys. Rev. A* **87** 010102
[12] Galleani L and Tavella P 2010 *IEEE Control Syst. Mag.* **30** 44
[13] Tavella P and Thomas C 1991 *Metrologia* **28** 57
[14] Wang F M, Chen Y F, Zhou J H, Lin Y T, Yang J, Wang B and Wang L J 2024 *Chin. Phys. B* **33** 010702
[15] Liu Y, Xu B, Yin J, Shen D, Ouyang M J, Zheng Z H and Zhu X W 2022 *Metrologia* **59** 035009
[16] Parker T E 2012 *Rev. Sci. Instrum.* **83** 021102
[17] Guo Y C, Wang B, Wang F M, Shi F F, Zhang A M, Zhu X, Yang J, Feng K M, Han C H, Li T C and Wang L J 2019 *Metrologia* **56** 045003
[18] Lee S W 2009 *Metrologia* **46** 693
[19] Azoubib J, Nawrocki J and Lewandowski W 2003 *Metrologia* **40** S245
[20] Levine J 2008 *Metrologia* **45** S23
[21] Sherman J A, *et al.* 2021 *NIST Technical Note* 2187
[22] Liu Y, Xu B, Yin J, Shen D, Ouyang M J, Zheng Z H and Zhu X W 2022 *Metrologia* **59** 035009
[23] Wang X B, Han C H and Yang Y X 2023 *GPS Solut.* **27** 1
[24] Weiss M and Weissert T 1991 *Metrologia* **28** 65
[25] Weiss M A, Allan D W and Peppler T K 1989 *IEEE Trans. Instrum. Meas.* **38** 631
[26] Levine J 2012 *Rev. Sci. Instrum.* **83** 021101
[27] Tavella P, Azoubib J and Thomas C 1991 *Proceedings of the 5th European Frequency and Time Forum*, March 12–14, Besançon, France, p. 435
[28] Ma F M 1984 *Acta Metrol Sinica* **5** 28
[29] Wu Y W, Yang B, Xiao S H and Wang M L 2019 *Geomatics and Information Science of Wuhan University* **44** 1226
[30] Tavella P and Premoli A 1994 *Metrologia* **30** 479
[31] Torcaso F, Ekstrom C R, Burt E A and Matsakis D N 2000 *IEEE Trans. Ultrason. Ferroelectr. Freq. Control* **47** 1183
[32] Guo Y C, Wang B, Wang F M, Si H W, Zuo Y N and Wang L J 2019 *Joint Conference of the IEEE International Frequency Control Symposium and European Frequency and Time Forum (EFTF/IFCS)*, April 14–18, Orlando, FL, USA, p. 1
[33] Wang B, Gao C, Chen W L, Miao J, Zhu X, Bai Y, Zhang J W, Feng Y Y, Li T C and Wang L J 2012 *Sci. Rep.* **2** 556